Macromolecules

Article

Cite This: Macromolecules 2017, 50, 7872-7879

pubs.acs.org/Macromolecules

Electrochemically Mediated Reversible Addition−Fragmentation Chain-Transfer Polymerization

Yi Wang, Marco Fantin, Sangwoo Park, Eric Gottlieb, Liye Fu, and Krzysztof Matyjaszewski*

Department of Chemistry, Carnegie Mellon University, 4400 Fifth Avenue, Pittsburgh, Pennsylvania 15213, United States

Supporting Information

ABSTRACT: An electrochemically mediated reversible addition−fragmentation chain-transfer polymerization (*e*RAFT) of (meth)acrylates was successfully carried out via electroreduction of either benzoyl peroxide (BPO) or 4-bromobenzenediazonium tetrafluoroborate ($BrPhN_2^+$) which formed aryl radicals, acting as initiators for RAFT polymerization. Direct electroreduction of chain transfer agents was unsuccessful since it resulted in the formation of carbanions by a two-electron-transfer process. Reduction of $BrPhN_2^+$ under a fixed potential showed acceptable control but limited conversion due to the generation of a passivating organic layer grafted on the working electrode surface. However, by use of fixed current conditions, easier to implement than fixed potential conditions, conversions >80% were achieved. Well-defined homopolymers and block copolymers with a broad range of targeted degrees of polymerization were prepared.

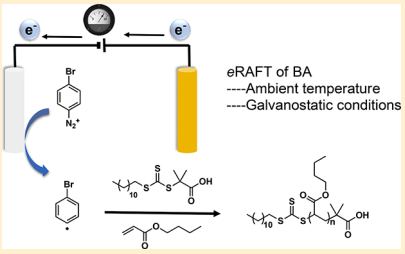

1. INTRODUCTION

Reversible deactivation radical polymerization (RDRP) methods have been employed to prepare polymers with predetermined molecular weight (MW), low dispersity (*Đ*), controlled architecture, and preserved chain-end functionality.[1] Reversible radical trapping and degenerative chain transfer ensure concurrent growth of all polymer chains and are employed to extend the lifetime of propagating chains from seconds to hours or even days.[1,2] Two most often used RDRP methods include atom transfer radical polymerization (ATRP)[3−6] and reversible addition−fragmentation radical polymerization (RAFT) polymerization.[7,8]

ATRP is based on converting propagating radicals ($P_n^\bullet$) into dormant alkyl halide species (P_n−X) by transition metal complexes, usually X−Cu^{II}/L (L = ligand) (Figure 1A).[3,5] The resulting Cu^I/L complex reactivates the dormant species, P_n−X. The dynamic exchange between active and dormant states enables the simultaneous and uniform growth of all chains with predetermined molecular weights and high chain-end fidelity.

In ATRP, the active Cu^I/L catalyst can be (re)generated by (photo)chemical or electrochemical methods.[9−13] Electrochemically mediated ATRP (*e*ATRP) relies on the well-defined and reversible redox behavior of Cu/L complexes (Figure 1B), which allows for a precise control of the polymerization. For example, the $[Cu^I]/[Cu^{II}]$ ratio can be set by adjusting the applied potential, which in turn determines the polymerization rate;[9,14] *e*ATRP can be switched "on" and "off" by shifting the potential during polymerization.[9,15] Moreover, Cu can be easily recycled by electroplating onto the working electrode (WE) and then oxidized back into solution and reused multiple times.[14,16] *e*ATRP has been applied to various monomers,[9,15,17] preparing copolymers with different architectures[18,19] in a range of reaction media.[20,21] Computational simulations were also conducted for *e*ATRP, elucidating the key parameters.[22] The application of Fe-based catalyst broadened the application of *e*ATRP.[23]

Another important RDRP procedure is RAFT polymerization (Figure 2),[8,24−27] which is based on degenerative transfer, and is mediated by chain transfer agents (CTAs) such as dithioesters, dithiocarbamates, trithiocarbonates, or xanthates.[25] RAFT polymerization is compatible with many vinyl

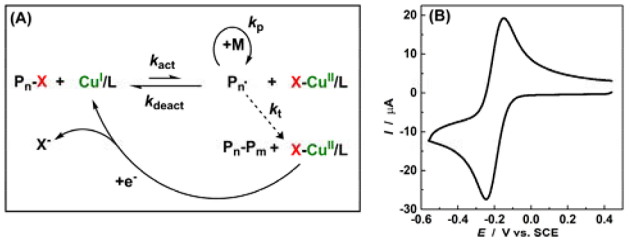

Figure 1. (A) Mechanism of *e*ATRP. (B) CV of 2×10^{-3} M [Br−Cu^{II}(tris(2-methylpyridyl)amine]$^+$ in DMSO + 0.1 M Et_4NBF_4, at T = 25 °C and scan rate 0.2 V s^{-1}.

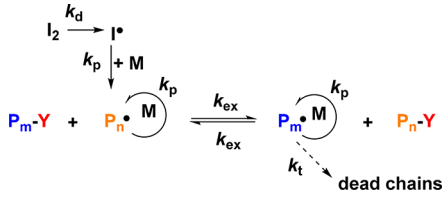

Figure 2. Mechanism of RAFT polymerization.

Received: September 15, 2017
Revised: October 3, 2017
Published: October 13, 2017

DOI: 10.1021/acs.macromol.7b02005
Macromolecules 2017, 50, 7872−7879

monomers and solvents, including both homogeneous and heterogeneous conditions.[28]

A continuous supply of radicals (i.e., "initiation") is essential in RAFT due to inevitable termination process. Initiation can be accomplished by thermal decomposition of radical sources such as azobis(isobutyronitrile) (AIBN) between 50 and 70 °C. However, such temperatures may be not suitable for some functional monomers[29] or for biological or thermoresponsive systems.[30] Thus, alternative radical generation methods were used for RAFT at ambient temperature, including zerovalent metals,[31−33] redox reactions,[34,35] γ-rays,[36] and light via the iniferter[37] or the photoinduced electron transfer processes.[38,39]

In this work, we investigated the use of electrical current for RAFT polymerization, inspired by successful *e*ATRP procedure and by modification of electrodes in the presence of RAFT agents.[40−42] However, an electrochemically mediated RAFT (*e*RAFT) is more challenging than *e*ATRP. Cu/L complexes for ATRP have a well-defined and reversible redox behavior,[43] whereas the electrochemical reactivity of RAFT agents is mostly unexplored and could result in irreversible redox processes that cannot be exploited to generate radicals. Thus, we first studied the redox properties of common CTAs (Figure 3B), which

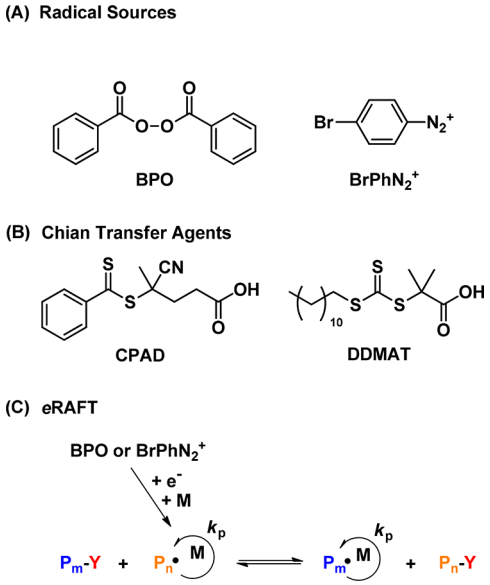

Figure 3. Structures of (A) radical sources and (B) CTAs used in this work. (C) Schematic representation of *e*RAFT polymerization, where Y is a chain-transfer moiety, M = monomer, and k_p = propagation rate constant.

were found to be unsuitable for the direct electrogeneration of radicals by reduction on common electrodes. To circumvent this limitation, we employed electroreduction of common radical initiators, such as benzoyl peroxide (BPO), or a diazonium salt, 4-bromobenzenediazonium tetrafluoroborate ($BrPhN_2^+$). As depicted in Figure 3C, reduction of both compounds generated radicals at ambient temperature, triggering controlled *e*RAFT polymerization of methyl methacrylate (MMA), *n*-butyl acrylate (BA), and *tert*-butyl acrylate (*t*BA).

Reduction of diazonium salts occurred at more positive potentials and was further investigated for eRAFT under both fixed potential and fixed current conditions. The rate of radical generation was controlled by electrical current or potential, providing well-defined polymers with variable degrees of polymerizations (DPs) and good retention of chain-end functionality.

2. RESULTS AND DISCUSSION

Electrochemical Properties of RAFT Chain Transfer Agents. Cyclic voltammetry (CV) of CPAD (4-cyano-4-(phenylcarbonothioylthio)pentanoic acid) and DDMAT (2-(dodecylthiocarbonothioylthio)-2-methylpropionic acid) gave irreversible reduction peaks at −1.00 and −1.25 V vs saturated calomel electrode (SCE) (Figure 4). These values are comparable to the ones obtained in a previous report.[44] Quantitative reduction of CPAD by electrolysis at −1.4 V vs SCE required two electrons per CPAD molecule (Figure S1). Both CV and electrolysis suggested that the weak C−S bond was irreversibly cleaved, with reduction of both ensuing fragments to anions, without generating radicals (eq 1). A

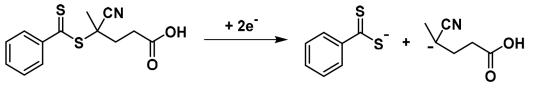

(1)

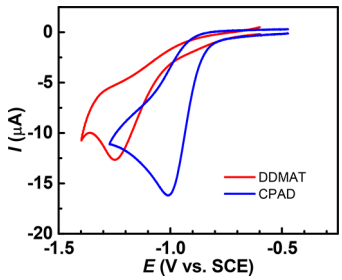

Figure 4. CV of 10^{-3} M CPAD and DDMAT in DMF + 0.1 M n-Bu_4NPF_6. T = 25 °C, v = 0.1 V s^{-1}.

similar behavior was observed for the reduction of alkyl halides used as ATRP initiators, which are also characterized by a weak bond, C−Br.[45] This mechanism is fundamentally different from the one-electron photoreduction in the photoinduced electron transfer (PET)-RAFT process.[39] Indeed, bulk electroreduction of the CTAs in the presence of monomer did not yield any polymer, confirming that the reduction process did not produce any long-lived free radicals. Therefore, electroreduction of radical initiators was tested in place of the electroreduction of CTAs.

Electrochemical Properties of Benzoyl Peroxide. Benzoyl peroxide (BPO) is a thermal initiator with a half-life time of ∼1 h at 90 °C.[46] However, BPO is essentially stable at ambient temperature and without application of any electrical current, giving <1% of MMA conversion after 20 h (Table 1, entry 1). CV showed that BPO is irreversibly reduced at cathodic peak potential $E_{pc,BPO}$ = −0.83 V vs SCE (Figure 5). The peak significantly overlapped with the reduction of CPAD ($E_{pc,CPAD}$ = −1.00 V vs SCE), which could be problematic due to concurrent electroreduction of CTA.

The overall electroreductive cleavage of BPO to two anionic fragments requires two electrons (eqs 2 and 3).[47] However, it involves the formation of more stable radical intermediates, which could initiate a polymerization in the presence of monomer (eq 4). Indeed, electroreduction of BPO at E_{app} = $E_{pc,BPO}$ − 0.08 V in the presence of MMA gave polymers in good yield via free radical polymerization (FRP, Figure S2, and Table 1, entry 2).

DOI: 10.1021/acs.macromol.7b02005
Macromolecules 2017, 50, 7872−7879

Table 1. *e*RAFT by Electroreduction of BPO[a]

entry	M	[M]/[CPAD]/[BPO]	E_{app}	time (h)	conv (%)	k_p^{app} [b] (h^{-1})	$M_{n,th}$ [c] ($\times 10^{-3}$)	$M_{n,app}$ ($\times 10^{-3}$)	M_w/M_n
1	MMA	500/0/1		20	1				
2	MMA	4670/0/1	$E_{pc,BPO}$ − 0.08 V	20	38	0.023		71.1	1.78
3	MMA	500/1/1	$E_{pc,BPO}$ − 0.17 V	20	<5				
4	MMA	500/1/1	$E_{pc,BPO}$ − 0.05 V	20	22	0.013	10.9	7.2	1.17
5	MMA	500/1/1	$E_{pc,BPO}$ + 0.34 V	20	0				
6[d]	BA	500/1/1	$E_{pc,BPO}$	20	25	0.015	10.0	7.6	1.16

[a][MMA] = 4.67 M (in DMF, 50% v/v), V_{tot} = 30 mL, [Et_4NPF_6] = 0.1 M, T = 25 °C. [b]The slope of the $\ln([M]_0/[M])$ vs time plot. [c]$M_{n,th}$ = [M]/[CTA] × M_M × conversion + M_{CTA}. [d]BA and DDMAT replaced MMA and CPAD.

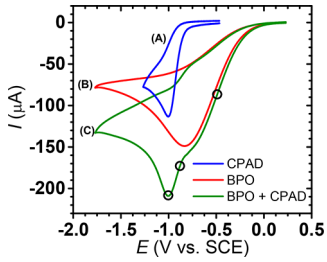

Figure 5. CV of (A) 7 × 10^{-3} M CPAD, (B) 10^{-2} M BPO, and (C) 7 × 10^{-3} M CPAD + 10^{-2} M BPO in DMF + 0.1 M Et_4NPF_6; T = 25 °C, v = 0.1 V s^{-1}. The circles represent E_{app} during polymerization.

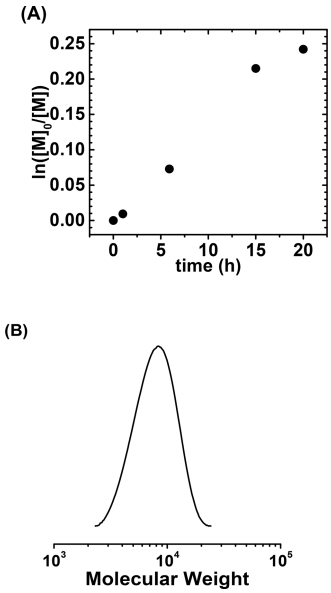

Figure 6. *e*RAFT of MMA by electroreduction of BPO. (A) Semilogarithmic kinetic plot and (B) gel permeation chromatography (GPC) of the obtained polymer, at E_{app} = $E_{pc,BPO}$ − 0.05 V (Table 1, entry 4). Reaction conditions: [MMA] = 4.67 M (in DMF, 50% v/v), V_{tot} = 30 mL, [MMA]/[CPAD]/[BPO] = 500/1/1, [Et_4NPF_6] = 0.1 M, T = 25 °C.

$$(RO)_2 + e^- = RO^\bullet + RO^- \quad (2)$$

$$RO^\bullet + e^- = RO^- \quad (3)$$

$$RO^\bullet + M = P_n^\bullet \quad (4)$$

***e*RAFT with BPO.** In the presence of CPAD and BPO, MMA was polymerized at three different applied potentials shown by the circles in Figure 5 (entries 3−5 in Table 1). At E_{app} = $E_{pc,BPO}$ − 0.17 V, <5% conversion was detected. The potential was too negative, resulting in decomposition of the CTA. At E_{app} = $E_{pc,BPO}$ − 0.05 V, controlled polymerization

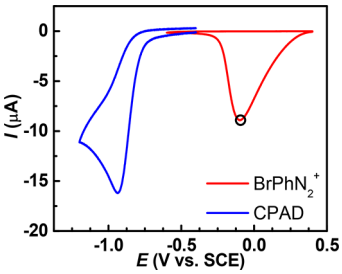

Figure 7. CV of 10^{-3} M $BrPhN_2^+$ and 10^{-3} M CPAD. The circle represent E_{app} during polymerization.

with a linear semilogarithmic kinetics and low $Đ$ was observed (Figure 6), but M_n was 30% lower than theoretical value due to chains generated by BPO "electrodecomposition". At E_{app} = $E_{pc,BPO}$ + 0.34 V, reduction of BPO was insufficient, and no polymer was generated. The large overlap between the reduction waves of CPAD and BPO narrowed the useful potential window to conduct an *e*RAFT; thus, only $E_{app} \approx E_{pc,BPO}$ could be successfully applied.

BA was also polymerized in the presence of DDMAT and BPO, at E_{app} = $E_{pc,BPO}$ (Table 1, entry 6). Despite the smaller overlap between the reduction waves of DDMAT and BPO, slow polymerization and M_n lower than theoretical values were observed. The limited potential window available with BPO prompted us to use a radical source with a more positive potential.

Electrochemical Properties of $BrPhN_2^+$. Reduction of $BrPhN_2^+$ gave an irreversible reduction peak at about −0.1 V vs SCE, which is ∼1 V more positive than reduction of CPAD (Figure 7). Therefore, $BrPhN_2^+$ could be reduced without affecting the CTAs. The reduction of $BrPhN_2^+$ is a well-known process that generates very reactive bromophenyl radicals ($BrPh^\bullet$). They are so reactive that they can quickly graft onto any electrode surface, forming a multilayered coating of branched bromobenzenes.[48] However, some radicals can escape to solution to initiate and sustain the RAFT polymerization. Only a small amount of radicals is required to sustain the process because radical concentration is typically low (<10^{-8} M). Therefore, we tested electrogeneration of radicals via reduction of $BrPhN_2^+$.

Electrogeneration of Radicals by $BrPhN_2^+$. FRP of BA was conducted by reducing $BrPhN_2^+$ at E_{app} = $E_{pc,BrPhN_2^+}$ on a Pt foil electrode (Table 2, entry 1). PBA was formed reaching 75% monomer conversion in 16 h and high molecular weight, M_n = 681 000 (Figure S5), typical for FRP. This confirmed that electroreduction of $BrPhN_2^+$ generated aryl radicals that could initiate polymerization significantly faster than with BPO.

Potentiostatic *e*RAFT with $BrPhN_2^+$. Potentiostatic *e*RAFT was conducted under a fixed E_{app} = $E_{pc,BrPhN_2^+}$ ≈ −0.1

DOI: 10.1021/acs.macromol.7b02005
Macromolecules 2017, 50, 7872−7879

Table 2. *e*RAFT of BA and MMA by Reduction of $BrPhN_2^+$ under Potentiostatic Conditions[a]

entry	M	time (h)	[M]/[DDMAT]/[$BrPhN_2^+$]	Q[b] (C)	conv (%)	k_p^{app}[c] (h^{-1})	$M_{n,th}$[d] ($\times10^{-3}$)	$M_{n,app}$ ($\times10^{-3}$)	M_w/M_n
1	BA	16	500/0/1	−0.5	75	0.087		681.0	1.44
2	BA	4	500/1/10	−11.6	60	0.248	38.9	18.9	6.23
3	BA	20	500/1/1	−7.0	48	0.183	31.1	24.4	1.27
4	BA	20	500/1/0.5	−6.0	25	0.079	16.3	13.8	1.15
5[e]	MMA	48	500/1/10	−0.5	40	0.017	20.0	19.8	1.20

[a][BA] = 3.49 M (in DMF, 50% by v/v), V_{tot} = 8 mL, WE = Pt mesh (except for entry 1: Pt foil), E_{app} = −0.1 V vs SCE. E_{app} was close to E_{pc} of the irreversible reduction peak of $BrPhN_2^+$. [b]Consumed charge, calculated from cathodic current profile recorded during electrolysis. [c]The slope of the $\ln([M]_0/[M])$ vs time plot. k_{app} for entries 2−4 was measured in the first 4 h. [d]$M_{n,th}$ = [M]/[CTA] × M_M × conversion + M_{CTA}. [e]MMA = 4.67 M in DMF (Figure S7).

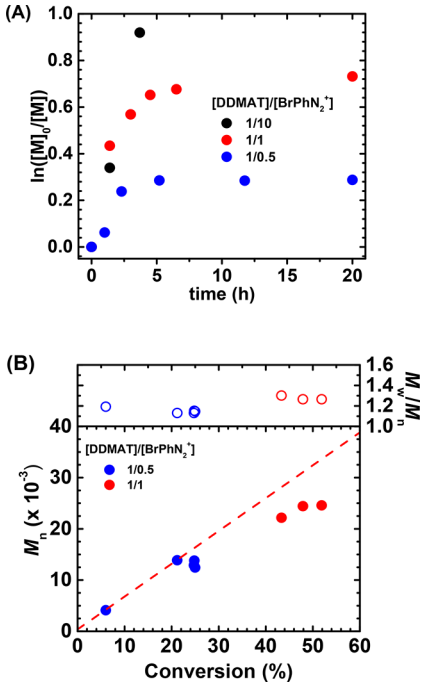

Figure 8. *e*RAFT of BA under potentiostatic conditions. (A) Polymerization kinetics. (B) MW and Đ evolution with conversion. Reaction conditions: [BA] = 3.49 M (in DMF, 50 vol %), [BA]/[DDMAT] = 500/1, [Et_4NPF_6] = 0.1 M, T = 25 °C, E_{app} = −0.1 V vs SCE.

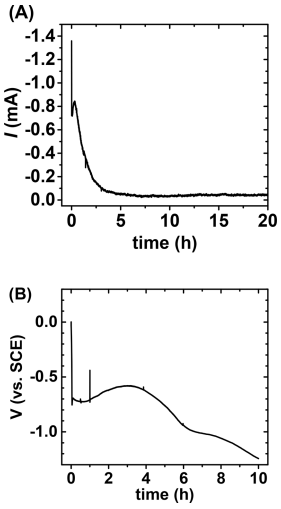

Figure 9. *e*RAFT by electroreduction of 7 × 10^{-3} M $BrPhN_2^+$: (A) current profile during chronoamperometry at E_{app} = $E_{pc,BrPhN_2^+}$ (Table 2, entry 3) and (B) potential between WE and CE during chronopotentiometry at I_{app} = −50 uA (Table 4, entry 3).

Table 3. XPS of Pt Foil Electrode before and after Electrochemical Reduction of $BrPhN_2^+$ [a]

atom number %	O	C	Pt	Br
before reaction	37.6	34.4	38.0	0
after 2 h reaction	20.7	74.9	2.8	1.6

[a]The large amount of adventitious O and C on the surface prior to deposition is due to the process employed to clean and activate the Pt electrode surface (see Supporting Information).

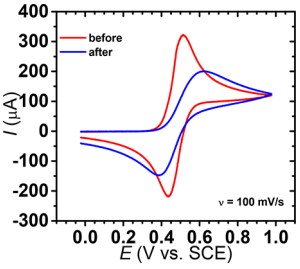

Figure 10. CV of 10^{-2} M ferrocene (red) before and (blue) after grafting of aryl compounds. The grafting was performed by CV of 7 × 10^{-3} M $BrPhN_2^+$ between +0.3 and −0.3 V vs SCE. WE = Pt disk in DMF + 0.1 M Et_4NPF_6 at 25 °C.

V vs SCE, using DDMAT as chain transfer agent for BA polymerization. Figure 8 shows the influence of the [DDMAT]/[$BrPhN_2^+$] ratio on *e*RAFT. The rate of polymerization increased with [$BrPhN_2^+$] due to faster reduction, which led to a higher concentration of radicals. However, the addition of too much diazonium salt was detrimental to polymerization control. The final M_w/M_n was 6.2 for [DDMAT]/[$BrPhN_2^+$] = 1/10 (Table 2, entry 2), whereas M_w/M_n was 1.3 for [DDMAT]/[$BrPhN_2^+$] = 1/1.

Despite the better control over Đ, the final MW was 15% lower than the theoretical value, suggesting that reduction of $BrPhN_2^+$ generated more chains than defined by DDMAT. Continuous generation of new chains during polymerization caused some low MW tailing and higher dispersity. Decreasing the [DDMAT]/[$BrPhN_2^+$] to 0.5 improved control, but polymerization was slower (Figure 8).

For [$BrPhN_2^+$]/[DDMAT] = 1/1 and 1/0.5, the reaction stopped after ca. 5 h at limited conversion (Figure 8A). This could be due to insufficient current flowing from the working electrode. Indeed, at fixed E_{app} the applied current quickly decayed (Figure 9A) due to electrografting of the insulating aryl compounds, as discussed in the next section.

DOI: 10.1021/acs.macromol.7b02005
Macromolecules 2017, 50, 7872−7879

Table 4. Galvanostatic *e*RAFT with $BrPhN_2^+$ [a]

entry	time (h)	I_{app} (μA)	Q^b (C)	conv (%)	$k_p^{app\,c}$ (h^{-1})	$M_{n,th}{}^d$ ($\times10^{-3}$)	$M_{n,app}$ ($\times10^{-3}$)	M_w/M_n
1	10	−200	−7.2	80	0.186	51.5	27.9	1.41
2	10	−100	−3.6	73	0.160	47.1	32.4	1.25
3	10	−50	−1.8	58	0.099	37.5	33.4	1.18

[a]General reaction conditions: [BA] = 3.49 M (in DMF, 50% by v/v), V_{tot} = 8 mL, [BA]/[DDMAT]/[$BrPhN_2^+$] = 500/1/1, [Et_4NPF_6] = 0.1 M, T = 25 °C. [b]Calculated from cathodic current profile recorded during electrolysis. [c]The slope of the $\ln([M]_0/[M])$ vs time plot. [d]$M_{n,th}$ = [M]/[CTA] × M_M × conversion + M_{CTA}.

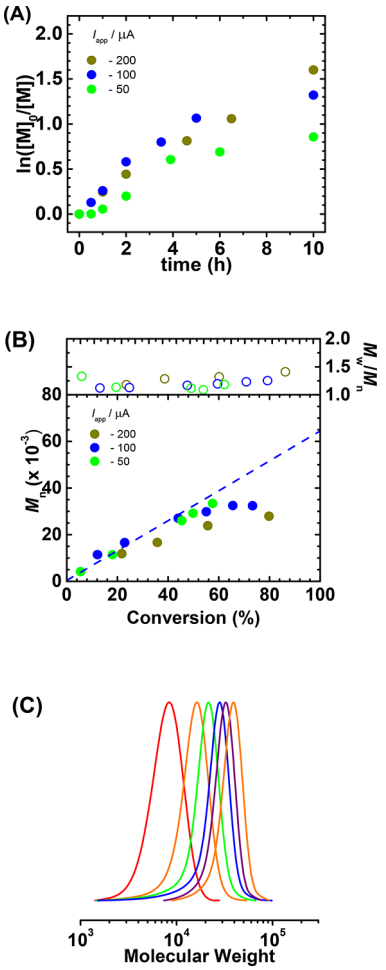

Figure 11. Galvanostatic *e*RAFT of BA with different I_{app}s. Reaction conditions: [BA] = 3.49 M (in DMF, 50 vol %), [BA]/[DDMAT]/[$BrPhN_2^+$] = 500/1/1, [Et_4NPF_6] = 0.1 M, T = 25 °C. (A) Kinetic plot; (B) evolution of MW and $Đ$; (C) GPC traces for I_{app} = −50 μA.

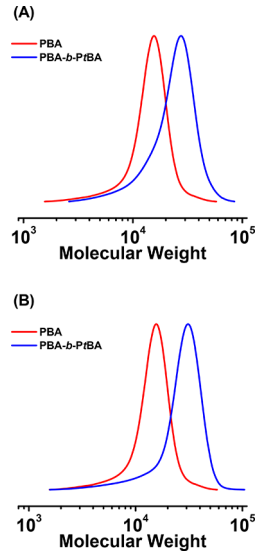

Figure 12. Chain extension of PBA-macroCTA with *t*BA by (A) *e*RAFT at room temperature and (B) RAFT polymerization initiated by AIBN at 65 °C.

*e*RAFT of MMA was also examined at fixed E_{app} and in the presence of CPAD. Despite a slow polymerization rate, the MW of the resulting PMMA correlated well with theoretical values and $Đ$ was 1.2 (Table 2, entry 5, and Figure S7). Interestingly, almost identical polymerization results were obtained for three different working electrodes, Pt, carbon felt, or graphite (Figures S7−S9). Polymers with higher $Đ$ were obtained when using a Cu electrode (Figure S10).

Electrografting of Aryl Compounds. The low current and slow polymerization rate observed under potentiostatic conditions prompted us to analyze the electrografting of $BrPhN_2^+$ on the surface of the WE. A variety of surfaces such as carbon, metals, and semiconductors can be grafted via a reduction of diazonium salts.[39,40] They are important agents for surface modification.[49−55] Even in the presence of monomer, a large fraction of aryl radicals were grafted onto the electrode, while some of them initiated polymerization. Although polymeric radicals cannot directly graft onto the electrode, they could covalently couple to the grafted aryl rings in the 3- or 5-position, thus increasing the thickness of organic layer.[50,56]

The layer grafted during electrochemical FRP of BA (conditions as in Table 2, entry 1) was analyzed by X-ray photoelectron spectroscopy (XPS). XPS of the Pt WE showed an increase in the presence of C and Br, demonstrating grafting of an organic layer containing bromoaryl groups (Table 3 and Figure S11). The Pt content on the surface strongly decreased, indicating almost complete coverage; about 3% of Pt remained exposed, allowing for continuous electroreduction throughout the process. The macroscopic appearance of the electrode did not change after polymerization, indicating the formation of a thin layer.

The Pt surface was also investigated by CV of a redox probe, ferrocene, which was analyzed before and after reduction of the diazonium salt (Figure 10). After deposition, ΔE_p (the difference between anodic and cathodic peak potentials) increased. This indicated the presence of a layer that decreased the rate of electron transfer to ferrocene on the surface. The resistance caused by the organic layer dissipated some of the applied voltage, lowering the true applied potential in the polymerization, so that true potentiostatic conditions were not applied. This explains the decreasing polymerization rate in Figure 8A. In conclusion, the electrografting of a poorly conductive layer on the electrode slowed $BrPhN_2^+$ reduction, leading to current decay and slower radical generation.

DOI: 10.1021/acs.macromol.7b02005
Macromolecules 2017, 50, 7872−7879

Table 5. Chain Extension of PBA-MacroCTA by *e*RAFT and Conventional RAFT Polymerization

entry	time (h)	[*t*BA]/[PBA-macroCTA]/[I]	I_{app} (μA)	Q^a (C)	conv (%)	$k_p^{app\,b}$ (h^{-1})	$M_{n,th}{}^c$ ($\times10^{-3}$)	$M_{n,app}$ ($\times10^{-3}$)	M_w/M_n
1[d]	5	500/1/1	−50	−0.9	22	0.040	26.8	20.2	1.27
2[e]	2	500/1/0.2			25	0.135	28.8	22.4	1.29

[a]Calculated from cathodic current profile recorded during electrolysis. [b]The slope of the $\ln([M]_0/[M])$ vs time plot. [c]$M_{n,th} = [M]/[CTA] \times M_M \times$ conversion + M_{CTA}. [d]Reaction conditions: [*t*BA] = 3.4 M (in DMF, 50% by v/v), V_{tot} = 8 mL, I = $BrPhN_2^+$, [Et_4NPF_6] = 0.1 M, *T* = 25 °C, WE = Pt mesh, I_{app} = −100 μA. [e]Reaction conditions: [*t*BA] = 3.4 M (in DMF, 50% by v/v), V_{tot} = 8 mL, I = AIBN, *T* = 65 °C.

Galvanostatic *e*RAFT with $BrPhN_2^+$. Because of electrografting, potentiostatic conditions for eRAFT resulted in limited conversion. Therefore, polymerizations under a fixed current, i.e., galvanostatic conditions, were tested to provide a continuous supply of radicals. The setup was simple, with application of a single current step during each polymerization (in comparison, a galvanostatic *e*ATRP requires a few different current steps).[19,57] In *e*RAFT with $BrPhN_2^+$, however, the formation of a resistive organic layer required the application of a negative E_{app} to supply constant current during polymerization (Figure 9B). Despite the negative E_{app}, reduction of monomer or solvent is not significant (see Figures S16 and S17).

Different applied currents (I_{app}s) were tested, which affected rate of radical generation (Table 4, entries 1−3, and Figure S12). Increasing I_{app} from −50, to −100, and to −200 μA gave more linear semilogarithmic kinetic plots, and conversion reached 80% in 10 h with the highest I_{app} (Figure 11). This is a noticeable improvement compared to *e*RAFT under potentiostatic conditions, indicating that a fixed current can provide a more efficient supply of radicals.

I_{app} influenced also MW and *Đ*. At each applied current $M_{n,app} < M_{n,th}$, indicating the formation of new chains during polymerization. Higher I_{app} generated a larger numbers of chains compared to the number defined by the chain transfer agent and thus resulted in lower $M_{n,app}$.[58] Nevertheless, polymers with different degrees of polymerization were successfully prepared, in the range 100−400, with <30% deviation from theoretical DP and $M_w/M_n \approx 1.2$ (Table S1 and Figures S13, S14).

Chain Extension. To evaluate the chain-end functionality of the obtained PBA, a PBA-macroCTA was chain-extended with *t*BA (Figure 12). The PBA-macroCTA was prepared via galvanostatic *e*RAFT with $BrPhN_2^+$ (details in the Supporting Information) and had $M_{n,app}$ = 12 900 ($M_{n,th}$ = 13 200) and M_w/M_n = 1.19. The chain extension was carried out by both *e*RAFT and traditional RAFT polymerization. In the latter case, a thermal initiator, AIBN, was used at 65 °C (Table 5).

Figure 12 shows the GPC traces of the macroCTA and the resulting block copolymers (PBA-*b*-P*t*BA). The block copolymer obtained from *e*RAFT had $M_{n,app}$ = 20 200 ($M_{n,th}$ = 26 800) and M_w/M_n = 1.27, while the product obtained by extension with conventional RAFT polymerization had $M_{n,app}$ = 22 400 ($M_{n,th}$ = 28 800) and M_w/M_n = 1.29. In both cases, a clean shift of MWD with conversion was observed. Chain extension by *e*RAFT showed a larger fraction of low-MW chains, further indicating that new chains were initiated during polymerization by the *e*RAFT process. Nevertheless, chain extension by traditional RAFT showed that the initiator prepared by *e*RAFT retained most of its chain-end functionality.

3. CONCLUSIONS

An *e*RAFT polymerization was mediated by reduction of BPO or $BrPhN_2^+$ at a Pt electrode. The two initiators had very different reduction peak potentials, −0.83 and −0.10 V vs SCE, respectively. The CTAs were irreversibly reduced at peak potential ∼−1 V vs SCE via a two-electron reduction without formation of long-lived radical species; they could not be directly used to produce radicals by electroreduction.

Electroreduction of BPO initiated a conventional free radical polymerization and was used for a successful but slow *e*RAFT at potentials $E_{app} \approx E_{pc,BPO}$. Reduction of BPO partially overlapped with reduction of the CTAs, limiting the use of the peroxide for *e*RAFT polymerization.

Reduction of $BrPhN_2^+$ occurred at much more positive potentials than reduction of the CTAs, resulting in a more effective generation of radicals to initiate a RAFT polymerization. An undesired electrografting of the aryl radicals on the electrode surface decreased its conductivity.

Well-defined polymers were prepared by applying either fixed potential or fixed current conditions. *e*RAFT with $BrPhN_2^+$ can be carried out under galvanostatic conditions at a single current value, utilizing a simple current generator at ambient temperature. The amount of new chains generated by reduction of $BrPhN_2^+$ was lowered by decreasing I_{app} or by decreasing the amount of diazonium salt relative to the CTA. Lower I_{app}s produced better controlled polymers but at slower rates. The chain-end functionality was well-maintained, as confirmed by synthesis of block copolymers with narrow molecular weight distribution.

■ ASSOCIATED CONTENT

Supporting Information

The Supporting Information is available free of charge on the ACS Publications website at DOI: 10.1021/acs.macromol.7b02005.

Experimental details and polymerization results (PDF)

■ AUTHOR INFORMATION

Corresponding Author

*(K.M.) E-mail km3b@andrew.cmu.edu.

ORCID

Yi Wang: 0000-0002-4002-9516

Krzysztof Matyjaszewski: 0000-0003-1960-3402

Notes

The authors declare no competing financial interest.

■ ACKNOWLEDGMENTS

The support from the National Science Foundation (CHE 1707490) and the National Institutes of Health (R01DE020843) is acknowledged.

■ REFERENCES

(1) Braunecker, W. A.; Matyjaszewski, K. Controlled/living radical polymerization: Features, developments, and perspectives. *Prog. Polym. Sci.* **2007**, *32*, 93−146.

DOI: 10.1021/acs.macromol.7b02005
Macromolecules 2017, 50, 7872−7879

(2) Goto, A.; Fukuda, T. Kinetics of living radical polymerization. *Prog. Polym. Sci.* **2004**, *29*, 329−385.
(3) Wang, J. S.; Matyjaszewski, K. Controlled Living Radical Polymerization - Halogen Atom-Transfer Radical Polymerization Promoted by a Cu(I)/Cu(II) Redox Process. *Macromolecules* **1995**, *28*, 7901−7910.
(4) Wang, J. S.; Matyjaszewski, K. Controlled Living Radical Polymerization - Atom-Transfer Radical Polymerization In the Presence Of Transition-Metal Complexes. *J. Am. Chem. Soc.* **1995**, *117*, 5614−5615.
(5) Matyjaszewski, K. Atom Transfer Radical Polymerization (ATRP): Current Status and Future Perspectives. *Macromolecules* **2012**, *45*, 4015−4039.
(6) Matyjaszewski, K.; Xia, J. H. Atom transfer radical polymerization. *Chem. Rev.* **2001**, *101*, 2921−2990.
(7) Chiefari, J.; Chong, Y. K.; Ercole, F.; Krstina, J.; Jeffery, J.; Le, T. P. T.; Mayadunne, R. T. A.; Meijs, G. F.; Moad, C. L.; Moad, G.; Rizzardo, E.; Thang, S. H. Living free-radical polymerization by reversible addition-fragmentation chain transfer: The RAFT process. *Macromolecules* **1998**, *31*, 5559−5562.
(8) Moad, G.; Rizzardo, E.; Thang, S. H. Living Radical Polymerization by the RAFT Process - A Third Update. *Aust. J. Chem.* **2012**, *65*, 985−1076.
(9) Magenau, A. J. D.; Strandwitz, N. C.; Gennaro, A.; Matyjaszewski, K. Electrochemically Mediated Atom Transfer Radical Polymerization. *Science* **2011**, *332*, 81−84.
(10) Chmielarz, P.; Fantin, M.; Park, S.; Isse, A. A.; Gennaro, A.; Magenau, A. J. D.; Sobkowiak, A.; Matyjaszewski, K. Electrochemically mediated atom transfer radical polymerization (*e*ATRP). *Prog. Polym. Sci.* **2017**, *69*, 47−78.
(11) Pan, X. C.; Tasdelen, M. A.; Laun, J.; Junkers, T.; Yagci, Y.; Matyjaszewski, K. Photomediated controlled radical polymerization. *Prog. Polym. Sci.* **2016**, *62*, 73−125.
(12) Wang, Z. H.; Pan, X. C.; Yan, J. J.; Dadashi-Silab, S.; Xie, G. J.; Zhang, J. N.; Wang, Z. H.; Xia, H. S.; Matyjaszewski, K. Temporal Control in Mechanically Controlled Atom Transfer Radical Polymerization Using Low ppm of Cu Catalyst. *ACS Macro Lett.* **2017**, *6*, 546−549.
(13) Simakova, A.; Averick, S. E.; Konkolewicz, D.; Matyjaszewski, K. Aqueous ARGET ATRP. *Macromolecules* **2012**, *45*, 6371−6379.
(14) Magenau, A. J. D.; Bortolamei, N.; Frick, E.; Park, S.; Gennaro, A.; Matyjaszewski, K. Investigation of Electrochemically Mediated Atom Transfer Radical Polymerization. *Macromolecules* **2013**, *46*, 4346−4353.
(15) Fantin, M.; Isse, A. A.; Venzo, A.; Gennaro, A.; Matyjaszewski, K. Atom Transfer Radical Polymerization of Methacrylic Acid: A Won Challenge. *J. Am. Chem. Soc.* **2016**, *138*, 7216−7219.
(16) Jasinski, N.; Lauer, A.; Stals, P. J. M.; Behrens, S.; Essig, S.; Walther, A.; Goldmann, A. S.; Barner-Kowollik, C. Cleaning the Click: A Simple Electrochemical Avenue for Copper Removal from Strongly Coordinating Macromolecules. *ACS Macro Lett.* **2015**, *4*, 298−301.
(17) Chmielarz, P.; Krys, P.; Park, S.; Matyjaszewski, K. PEO-*b*-PNIPAM copolymers via SARA ATRP and eATRP in aqueous media. *Polymer* **2015**, *71*, 143−147.
(18) Park, S.; Cho, H. Y.; Wegner, K. B.; Burdynska, J.; Magenau, A. J. D.; Paik, H. J.; Jurga, S.; Matyjaszewski, K. Star Synthesis Using Macroinitiators via Electrochemically Mediated Atom Transfer Radical Polymerization. *Macromolecules* **2013**, *46*, 5856−5860.
(19) Chmielarz, P.; Park, S.; Sobkowiak, A.; Matyjaszewski, K. Synthesis of beta-cyclodextrin-based star polymers via a simplified electrochemically mediated ATRP. *Polymer* **2016**, *88*, 36−42.
(20) Fantin, M.; Isse, A. A.; Gennaro, A.; Matyjaszewski, K. Understanding the Fundamentals of Aqueous ATRP and Defining Conditions for Better Control. *Macromolecules* **2015**, *48*, 6862−6875.
(21) Fantin, M.; Park, S.; Wang, Y.; Matyjaszewski, K. Electrochemical Atom Transfer Radical Polymerization in Miniemulsion with a Dual Catalytic System. *Macromolecules* **2016**, *49*, 8838−8847.
(22) Guo, J. K.; Zhou, Y. N.; Luo, Z. H. Kinetic insight into electrochemically mediated ATRP gained through modeling. *AIChE J.* **2015**, *61*, 4347−4357.
(23) Guo, J. K.; Zhou, Y. N.; Luo, Z. H. Kinetic Insights into the Iron-Based Electrochemically Mediated Atom Transfer Radical Polymerization of Methyl Methacrylate. *Macromolecules* **2016**, *49*, 4038−4046.
(24) Moad, G.; Chiefari, J.; Chong, Y. K.; Krstina, J.; Mayadunne, R. T. A.; Postma, A.; Rizzardo, E.; Thang, S. H. Living free radical polymerization with reversible addition-fragmentation chain transfer (the life of RAFT). *Polym. Int.* **2000**, *49*, 993−1001.
(25) Moad, G.; Rizzardo, E.; Thang, S. H. Living radical polymerization by the RAFT process. *Aust. J. Chem.* **2005**, *58*, 379−410.
(26) Moad, G.; Rizzardo, E.; Thang, S. H. Living radical polymerization by the RAFT process - A first update. *Aust. J. Chem.* **2006**, *59*, 669−692.
(27) Moad, G.; Rizzardo, E.; Thang, S. H. Living Radical Polymerization by the RAFT Process - A Second Update. *Aust. J. Chem.* **2009**, *62*, 1402−1472.
(28) Hill, M. R.; Carmean, R. N.; Sumerlin, B. S. Expanding the Scope of RAFT Polymerization: Recent Advances and New Horizons. *Macromolecules* **2015**, *48*, 5459−5469.
(29) Li, Y.; Yang, J.; Benicewicz, B. C. Well-controlled polymerization of 2-azidoethyl methacrylate at near room temperature and click functionalization Journal of Polymer Science Part A: Polymer Chemistry Volume 45, Issue 18. *J. Polym. Sci., Part A: Polym. Chem.* **2007**, *45*, 4300−4308.
(30) Convertine, A. J.; Lokitz, B. S.; Vasileva, Y.; Myrick, L. J.; Scales, C. W.; Lowe, A. B.; McCormick, C. L. Direct synthesis of thermally responsive DMA/NIPAM diblock and DMA/NIPAM/DMA triblock copolymers via aqueous, room temperature RAFT polymerization. *Macromolecules* **2006**, *39*, 1724−1730.
(31) Kwak, Y.; Nicolay, R.; Matyjaszewski, K. Synergistic Interaction Between ATRP and RAFT: Taking the Best of Each World. *Aust. J. Chem.* **2009**, *62*, 1384−1401.
(32) Nicolay, R.; Kwak, Y.; Matyjaszewski, K. A Green Route to Well-Defined High-Molecular-Weight (Co)polymers Using ARGET ATRP with Alkyl Pseudohalides and Copper Catalysis. *Angew. Chem., Int. Ed.* **2010**, *49*, 541−544.
(33) Gu, Y. W.; Zhao, J. F.; Liu, Q. Q.; Pan, X. Q.; Zhang, W.; Zhang, Z. B.; Zhu, X. L. Zero valent metal/RAFT agent mediated CRP of functional monomers at room temperature: a promising catalyst system for CRP. *Polym. Chem.* **2015**, *6*, 359−363.
(34) Martin, L.; Gody, G.; Perrier, S. Preparation of complex multiblock copolymers via aqueous RAFT polymerization at room temperature. *Polym. Chem.* **2015**, *6*, 4875−4886.
(35) Vandenbergh, J.; Schweitzer-Chaput, B.; Klussmann, M.; Junkers, T. Acid-Induced Room Temperature RAFT Polymerization: Synthesis and Mechanistic Insights. *Macromolecules* **2016**, *49*, 4124−4135.
(36) Barner, L.; Quinn, J. F.; Barner-Kowollik, C.; Vana, P.; Davis, T. P. Reversible addition-fragmentation chain transfer polymerization initiated with gamma-radiation at ambient temperature: an overview. *Eur. Polym. J.* **2003**, *39*, 449−459.
(37) Otsu, T. Iniferter concept and living radical polymerization. *J. Polym. Sci., Part A: Polym. Chem.* **2000**, *38*, 2121−2136.
(38) Shanmugam, S.; Xu, J. T.; Boyer, C. Photoinduced Electron Transfer-Reversible Addition-Fragmentation Chain Transfer (PET-RAFT) Polymerization of Vinyl Acetate and N-Vinylpyrrolidinone: Kinetic and Oxygen Tolerance Study. *Macromolecules* **2014**, *47*, 4930−4942.
(39) Xu, J. T.; Jung, K.; Atme, A.; Shanmugam, S.; Boyer, C. A Robust and Versatile Photoinduced Living Polymerization of Conjugated and Unconjugated Monomers and Its Oxygen Tolerance. *J. Am. Chem. Soc.* **2014**, *136*, 5508−5519.
(40) Tria, M. C. R.; Grande, C. D. T.; Ponnapati, R. R.; Advincula, R. C. Electrochemical Deposition and Surface-Initiated RAFT Polymer-

DOI: 10.1021/acs.macromol.7b02005
Macromolecules 2017, 50, 7872−7879

ization: Protein and Cell-Resistant PPEGMEMA Polymer Brushes. *Biomacromolecules* **2010**, *11*, 3422−3431.
(41) Grande, C. D.; Tria, M. C.; Jiang, G. Q.; Ponnapati, R.; Advincula, R. Surface-Grafted Polymers from Electropolymerized Polythiophene RAFT Agent. *Macromolecules* **2011**, *44*, 966−975.
(42) Bunsow, J.; Manz, M.; Vana, P.; Johannsmann, D. Electrochemically Induced RAFT Polymerization of Thermoresponsive Hydrogel Films: Impact on Film Thickness and Surface Morphology. *Macromol. Chem. Phys.* **2010**, *211*, 761−767.
(43) Fantin, M.; Lorandi, F.; Gennaro, A.; Isse, A. A.; Matyjaszewski, K. Electron Transfer Reactions in Atom Transfer Radical Polymerization. *Synthesis* **2017**, *49*, 3311−3322.
(44) Christmann, J.; Ibrahim, A.; Charlot, V.; Croutxe-Barghorn, C.; Ley, C.; Allonas, X. Elucidation of the Key Role of [Ru(bpy)(3)](2+) in Photocatalyzed RAFT Polymerization. *ChemPhysChem* **2016**, *17*, 2309−2314.
(45) Isse, A. A.; Mussini, P. R.; Gennaro, A. New Insights into Electrocatalysis and Dissociative Electron Transfer Mechanisms: The Case of Aromatic Bromides. *J. Phys. Chem. C* **2009**, *113*, 14983−14992.
(46) Odian, G. G. *Principles of polymerization*, 4th ed.; Wiley-Interscience: Hoboken, NJ, 2004; p *xxiv*, 812 pp.
(47) Antonello, S.; Musumeci, M.; Wayner, D. D. M.; Maran, F. Electroreduction of dialkyl peroxides. Activation-driving force relationships and bond dissociation free energies. *J. Am. Chem. Soc.* **1997**, *119*, 9541−9549.
(48) Menanteau, T.; Dias, M.; Levillain, E.; Downard, A. J.; Breton, T. Electrografting via Diazonium Chemistry: The Key Role of the Aryl Substituent in the Layer Growth Mechanism. *J. Phys. Chem. C* **2016**, *120*, 4423−4429.
(49) Mahouche-Chergui, S.; Gam-Derouich, S.; Mangeney, C.; Chehimi, M. M. Aryl diazonium salts: a new class of coupling agents for bonding polymers, biomacromolecules and nanoparticles to surfaces. *Chem. Soc. Rev.* **2011**, *40*, 4143−4166.
(50) Deniau, G.; Azoulay, L.; Bougerolles, L.; Palacin, S. Surface electroinitiated emulsion polymerization: Grafted organic coatings from aqueous solutions. *Chem. Mater.* **2006**, *18*, 5421−5428.
(51) Belanger, D.; Pinson, J. Electrografting: a powerful method for surface modification. *Chem. Soc. Rev.* **2011**, *40*, 3995−4048.
(52) Bernard, M. C.; Chausse, A.; Cabet-Deliry, E.; Chehimi, M. M.; Pinson, J.; Podvorica, F.; Vautrin-Ul, C. Organic layers bonded to industrial, coinage, and noble metals through electrochemical reduction of aryldiazonium salts. *Chem. Mater.* **2003**, *15*, 3450−3462.
(53) Boukerma, K.; Chehimi, M. M.; Pinson, J.; Blomfield, C. X-ray photoelectron spectroscopy evidence for the covalent bond between an iron surface and aryl groups attached by the electrochemical reduction of diazonium salts. *Langmuir* **2003**, *19*, 6333−6335.
(54) Chausse, A.; Chehimi, M. M.; Karsi, N.; Pinson, J.; Podvorica, F.; Vautrin-Ul, C. The electrochemical reduction of diazonium salts on iron electrodes. The formation of covalently bonded organic layers and their effect on corrosion. *Chem. Mater.* **2002**, *14*, 392−400.
(55) Matrab, T.; Chehimi, M. M.; Perruchot, C.; Adenier, A.; Guillez, A.; Save, M.; Charleux, B.; Cabet-Deliry, E.; Pinson, J. Novel approach for metallic surface-initiated atom transfer radical polymerization using electrografted initiators based on aryl diazonium salts. *Langmuir* **2005**, *21*, 4686−4694.
(56) Tessier, L.; Deniau, G.; Charleux, B.; Palacin, S. Surface Electroinitiated Emulsion Polymerization (SEEP): A Mechanistic Approach. *Chem. Mater.* **2009**, *21*, 4261−4274.
(57) Fantin, M.; Lorandi, F.; Isse, A. A.; Gennaro, A. Sustainable Electrochemically-Mediated Atom Transfer Radical Polymerization with Inexpensive Non-Platinum Electrodes. *Macromol. Rapid Commun.* **2016**, *37*, 1318−1322.
(58) Keddie, D. J. A guide to the synthesis of block copolymers using reversible-addition fragmentation chain transfer (RAFT) polymerization. *Chem. Soc. Rev.* **2014**, *43*, 496−505.

DOI: 10.1021/acs.macromol.7b02005
Macromolecules 2017, 50, 7872−7879